Journal of Biomechanics 137 (2022) 111102

Contents lists available at ScienceDirect

Journal of Biomechanics

journal homepage: www.elsevier.com/locate/jbiomech

Skin marker-based subject-specific spinal alignment modeling: A feasibility study

Stefan Schmid [a,b,*,1], Lukas Connolly [c,d,e,1], Greta Moschini [c,e,f], Michael L. Meier [c,d], Marco Senteler [c,e,f]

[a] Bern University of Applied Sciences, Department of Health Professions, Division of Physiotherapy, Spinal Movement Biomechanics Group, Bern, Switzerland
[b] University of Basel, Faculty of Medicine, Basel, Switzerland
[c] University of Zurich, Balgrist University Hospital, Department of Chiropractic Medicine, Integrative Spinal Research, Zurich, Switzerland
[d] University of Zurich, Zurich, Switzerland
[e] ETH Zurich, Department of Health Science and Technology, Institute for Biomechanics, Zurich, Switzerland
[f] University of Zurich, Balgrist University Hospital, Department of Orthopedics, Zurich, Switzerland

ARTICLE INFO

Keywords:
Musculoskeletal modeling
Full-body
Spine
Functional activities

ABSTRACT

Musculoskeletal models have the potential to improve diagnosis and optimize clinical treatment by predicting accurate outcomes on an individual basis. However, the subject-specific modeling of spinal alignment is often strongly simplified or is based on radiographic assessments, exposing subjects to unnecessary radiation.

We therefore developed and introduced a novel skin marker-based approach for modeling subject-specific spinal alignment and evaluated its feasibility by comparing the predicted L1/L2 spinal loads during various functional activities with the loads predicted by the generically scaled models as well as with in vivo measured data obtained from the OrthoLoad database.

Spinal loading simulations resulted in considerably higher compressive forces for both scaling approaches over all simulated activities, and AP shear forces that were closer or similar to the in vivo data for the subject-specific approach during upright standing activities and for the generic approach during activities that involved large flexions.

These results underline the feasibility of the proposed method and associated workflow for inter- and intra-subject investigations using musculoskeletal simulations. When implemented into standard model scaling workflows, it is expected to improve the accuracy of muscle activity and joint loading simulations, which is crucial for investigations of treatment effects or pathology-dependent deviations.

1. Introduction

Musculoskeletal models and computer simulations are increasingly used for investigating biomechanical parameters that are difficult to assess experimentally (Bassani and Galbusera, 2018). The two most commonly used musculoskeletal modeling platforms are OpenSim (Delp et al., 2007) and AnyBody (AnyBody Technology, Arlborg, Denmark). While AnyBody is a commercial software, OpenSim is a free open-source modeling and simulation framework, which includes a growing database of models developed and published by various researchers (Bassani and Galbusera, 2018; Seth et al., 2011). For both platforms, various spine models are available, including models with only articulated lumbar spines (Christophy et al., 2012; de Zee et al., 2007) as well as models with fully articulated thoracolumbar spines and rib cages (Bruno et al., 2015; Ignasiak et al., 2016).

For simulating dynamic activities, these models are usually driven by skin marker-based motion capture data using an inverse kinematics approach (Bassani et al., 2017; Beaucage-Gauvreau et al., 2019; Glover et al., 2021; Ignasiak et al., 2018; Raabe and Chaudhari, 2018). But besides calculating joint angles during dynamic activities, marker data are also used for generic model scaling to account for subject-specific geometries and masses of the individual segments. These scaling procedures are based on a minimization approach, which in almost any case leads to a certain number of residual errors (Glover et al., 2021). It

* Corresponding author at: Bern University of Applied Sciences, Department of Health Professions, Murtenstrasse 10, 3008 Bern, Switzerland.
E-mail address: stefanschmid79@gmail.com (S. Schmid).
[1] These authors contributed equally.

https://doi.org/10.1016/j.jbiomech.2022.111102
Accepted 20 April 2022
Available online 25 April 2022
0021-9290/© 2022 The Author(s). Published by Elsevier Ltd. This is an open access article under the CC BY license (http://creativecommons.org/licenses/by/4.0/).

source: https://doi.org/10.24451/arbor.16975 | downloaded: 25.4.2024

particularly leads to inaccuracies when applied to the spine, which by itself is a multi-joint complex consisting of 24 vertebral bodies, with each having its own dimension and anatomical arrangement. Moreover, the dimensions of the rigid bodies representing the vertebrae are considerably smaller and driven by fewer markers than other body segments such as the extremities. Hence, the definition of spinal alignment based on skin markers represents an underdetermined geometrical problem. On the other hand, the spinal segments (and spinal markers) do not move independently but can be considered a kinematic chain with a large number of degrees of freedom. Consequently, standard personalization strategies in musculoskeletal spine modeling typically compromises subject-specific anatomical differences and neglects skeletal alignments in the spinal region.

To address these issues, we aimed at developing and introducing a novel approach for modeling subject-specific spinal alignment, which fully relies on skin marker data instead of data extracted from radiographic examinations. In addition, we aimed at evaluating its feasibility by conducting a proof-of-concept study, which includes the comparison of simulation outputs to in vivo measured spinal loading data obtained from a publicly available database.

2. Methods

2.1. Creating full-body models with subject-specific spinal alignment

2.1.1. Base models

All models were created using the OpenSim musculoskeletal modeling environment (Delp et al., 2007). As a basis for the development of subject-specific models, we created a set of male and female full-body models, composed of a fully articulated thoracolumbar spine model including a head-neck-complex and upper extremities (Bruno et al., 2015; Bruno et al., 2017) as well as the Gait2354 model (Anderson and Pandy, 1999; Anderson and Pandy, 2001; Delp et al., 1990; Yamaguchi and Zajac, 1989), a standard lower body model available from OpenSim. The models were scaled and combined as previously described (Burkhart et al., 2020; Schmid et al., 2020). To reduce complexity of the model and improve simulation robustness, external and internal intercostal muscle groups were removed, and ribs were considered as rigid bodies attached to the vertebrae. The axial rotation (AR) and lateral bending (LB) coordinates of the thoracic intervertebral joints (IVJs) were locked, reducing them to pin joints with one degree of freedom (flexion and extension (FE)). Additionally, the translational coordinates of the rib to sternum joints were locked, changing them from free to ball joints. To support the muscles (i.e. to account for synergistic passive structures such as the thoracolumbar fascia) and prevent the models from failing in tasks involving large ranges of motion (e.g. lifting up a box from the floor or standing up from a chair) or high impact forces (e.g. running or jumping), coordinate actuators (virtual torque generators) with infinite minimum and maximal control values were added to some joints. The FE, AR and LB coordinates of the L3/L4 to L5/S1 IVJs were thereby actuated with an optimal torque of 10 Nm, whereas the remaining lumbar IVJs (T12/L1 to L2/L3) were actuated with an optimal torque of 5 Nm and the FE coordinates of the thoracic IVJs with an optimal torque of 1 Nm. To further improve simulation robustness, the sternum to clavicle as well as the hip, knee and ankle joints were all actuated with an optimal torque of 25 Nm. These optimal torque were defined as large as needed for the model to converge and as small as possible to minimize the effect on the results. To compensate for the dynamic inconsistency between the estimated model accelerations and the measured ground reaction forces, residual actuators were added to all six degrees of freedom of the "pelvis to ground joint", which connects the model to the ground (i.e. to the origin of the coordinate system).

To allow for motion capture data-driven inverse kinematics calculations, we used the drag and drop OpenSim graphical user interface to add virtual markers, in a first step only to the male base model. We thereby chose the full-body marker set described by Schmid et al. (2017) (Fig. 1), mainly due to its demonstrated capacity for the reliable assessment of spinal kinematics during functional activities (Niggli et al., 2021; Suter et al., 2020). For all bilateral markers, the locations were mirrored to ensure a symmetric virtual marker set. To add the virtual markers also to the female base model, the marker offsets from the linked body segments were scaled with the same factor as used for scaling the respective body segment from the male to female model.

2.1.2. Generic model scaling

To account for individual segmental lengths and masses, base models are first selected according to the gender of the individual under investigation (subject) and scaled generically using the OpenSim scaling tool. This includes scaling of all segments by factors obtained from the distances between marker locations collected during an upright standing trial in the movement laboratory (Table 1). Static pose marker weights are 10.0 for the markers (R/L)ELB, (R/L)FIN, (R/L)KNE, (R/L)ANK and (R/L)TOE, and 1.0 for all remaining markers. Subsequently, the mass properties of the body segments are scaled while preserving mass distribution and reproducing the total mass (recorded using a standard bathroom scale) of the subject. Muscle properties such as fiber and tendon slack length are then scaled proportionally to the total muscle resting length. Additionally, virtual marker locations are adapted to match the experimental marker locations using the OpenSim scaling tool option 'Adjust Model Markers'.

2.1.3. Implementation of skin marker-derived spinal alignment

Following generic model scaling, spinal alignment is adjusted based on the external back profile of the subject using a custom MATLAB routine (R2020b, MathWorks, Inc., Natick, MA, USA). First, a 4th order polynomial is fitted through the sagittal plane coordinates of the markers placed over the spinous processes of C7, T3, T5, T7, T9, T11, L1-L5 and the sacrum (height of S2) (Fig. 2A). The sagittal plane is thereby defined by a plane fit into the locations of the 12 spinal markers (C7 to sacrum) as well as the markers placed on the sternum and bilaterally on claviculae. Through fitting the polynomial, potential discontinuities arising for example from marker (mis)placement are smoothed out by setting the horizontal (anterior-posterior) position of each marker as a result of the polynomial function of vertical (superior-inferior) position. Input points for the internal spinal alignment polynomial are then acquired by subtracting the scaled marker to joint center distance (in the base model) from the smoothened marker position. The underlying assumption thereby is a vertebral orientation along the normal vector of the external back profile polynomial at the height of the corresponding experimental marker (Fig. 2B). Exceptions are the predicted IVJ locations for the segments C7/T1 and T1/T2, since the "head and neck segment" (to which the C7 marker is linked to) is always oriented horizontally, and therefore, the T1/T2 IVJ location is calculated based on its offset from the C7 marker.

The sagittal plane projection of the geometric center between the two posterior head markers (located at the most posterior and lateral point of the head, approximately at the height of the temples) is added as a supporting point to account for an appropriate cervical lordosis. These points are then used to fit a second 4th order polynomial for predicting the internal spinal alignment (Fig. 2C). The estimated joint center locations in the sagittal plane are derived from the polynomial by setting the vertical position of each IVJ from the generically scaled base models as function input (Fig. 2D). The orientation of each vertebrae is derived from the angle of the normal vector at the joint center with respect to the frontal axis (Fig. 2E). Subject-specific pelvis orientation was not accounted for and therefore, sacrum and pelvis inclination of the subject-specific models remained the same as in the base models.

The estimated IVJ locations and orientations are then converted from global to local three-dimensional coordinate systems. Since the joint coordinate systems of the template model coincide with the centroids of the corresponding vertebral bodies, location and orientation of each

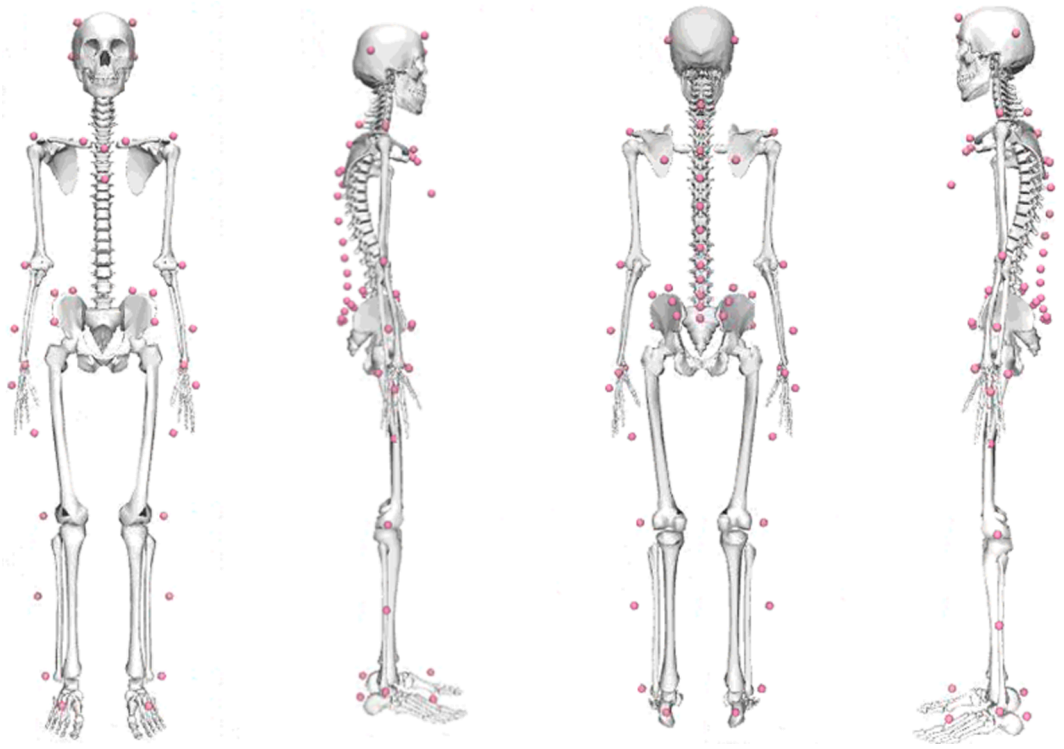

Fig. 1. The generic male full-body model with the 58 virtual markers according to the configuration described by Schmid et al. (2017).

Table 1
Reference marker pairs for generic model scaling. Marker names as well as marker placement locations correspond to the configuration described by Schmid et al. (2017).

Model region	Reference Marker Pairs	Scaled Bodies (X, Y, Z)
Torso	C7 → SACR	Pelvis, Sacrum, Abdomen, all Intervertebral Bodies, all Ribs, Sternum, Clavicles, Scapularies, Head / Neck
Upper extremities	RSHO → RFIN LSHO → LFIN	Humerus, Ulna, Radius, Hand (all bilateral)
Lower extremities	RASI → RANK LASI → LANK RKNE → RANK LKNE → LANK	Femur, Tibia, Talus, Calcaneus, Toes (all bilateral)

joint center are calculated with respect to the former joint in a global frame and converted to a local coordinate system by fixing each joint center in space and rotating the reference frame by its orientation angle. Additional model modifications such as rib and sternum relocation/reorientation are made to maintain the global distance and orientation from the base model to the modified spine. Center of mass locations for each spinal segment are readjusted to ensure the same relative position to the vertebral body. And finally, muscle fiber and tendon slack length are adjusted to match the proportions of the base model.

The OpenSim base models as well as the MATLAB code for subject-specific model scaling and spinal alignment adjustment are freely available via the project-hosting platform SimTK (https://simtk.org/projects/pers_fbm_spine).

2.2. Feasibility evaluation

To evaluate the feasibility of our subject-specific models for simulating spinal loading during functional activities, we conducted a proof-of-concept study, which was approved by the local ethics committee and for which all participants provided written informed consent. The study aimed at comparing the L1/L2 compressive and anterior-posterior (AP) shear forces predicted by the subject-specific models with the forces predicted by the generic models as well as with in vivo measured forces obtained from the OrthoLoad database (https://orthoload.com).

We therefore recruited 17 healthy individuals (13 males, 4 females; age: 28 ± 4.95 years; mass: 76.6 ± 10.4 kg; height: 179.3 ± 7.84 cm) and invited them for a single visit to our movement laboratory. After the acquisition of relevant anthropometric data (body mass, height), they were equipped with 58 retro-reflective skin markers in a configuration corresponding to the one implemented in the model (see section 2.1.1 and Fig. 1) and asked to stand upright for 10 s as well as to perform the functional activities walking, running (not evaluated in this study), lifting a 5 kg-box (box lifting), standing up from a chair (chair rising) and climbing stairs. Apart from standing upright, all tasks were performed five times. Motion data were recorded at a sampling rate of 200 Hz using a 27-camera optical motion capture system (Vicon, Oxford, UK). Recorded data were processed using the software Nexus (version 2.8.1, Vicon, Oxford, UK) and transformed into the OpenSim reference system using a custom MATLAB routine. Ground reaction forces were recorded at a sampling rate of 1 kHz using six level ground embedded force plates (AMTI, BP400600) and two mobile force plates (Kistler, 9260AA6) mounted on the first and second step of a four-step staircase.

Following data acquisition, subject-specific models were created based on the mean marker locations obtained during the first 5 s of the upright standing trial (see sections 2.1.2 and 2.1.3). For the box lifting task, a separate set of models was created by adding 2.5 kg to each hand and updating the inertial properties to account for the measures of the respective side of the box. No other model properties were changed for the box lifting task. For the walking and stair climbing tasks, start and stop events were set manually using the software Nexus, whereas for the chair rising and box lifting tasks, a custom MATLAB-based event detection algorithm was used. The start and the end of the two movements were thereby defined as the points where the vertical velocity of the C7 marker initially exceeded and fell below 5% of the maximal vertical velocity, respectively.

Simulations of spinal loading were carried out in three steps: (1)

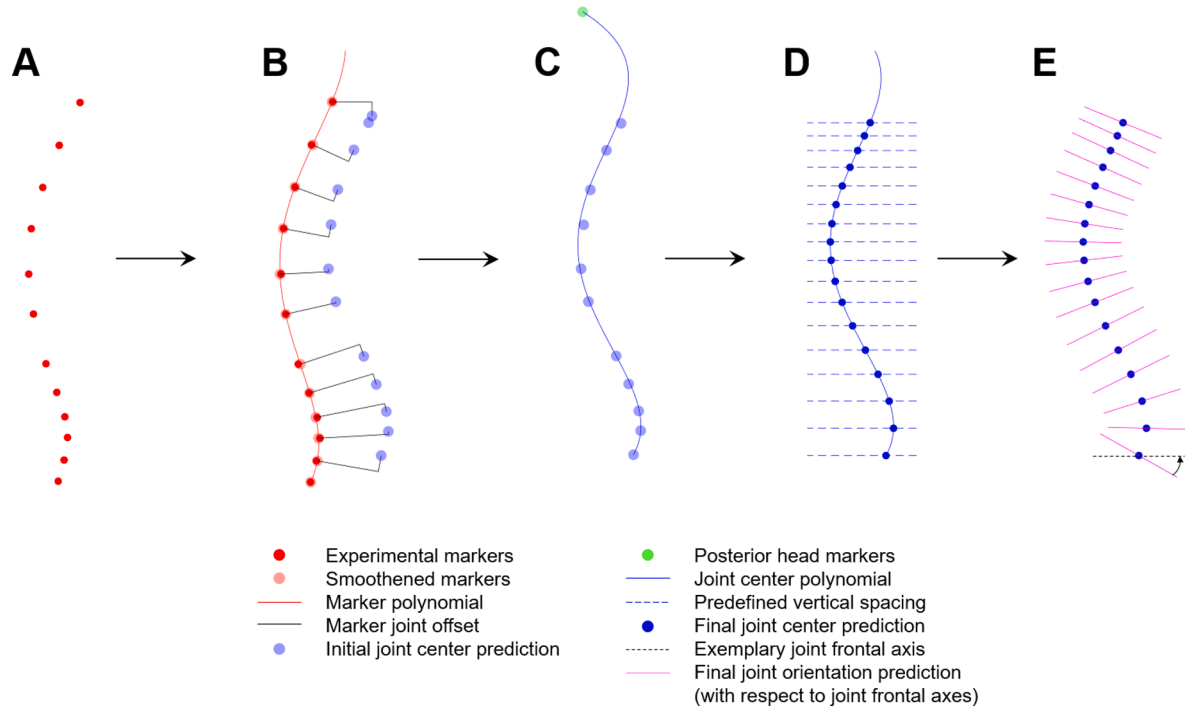

Fig. 2. Subject-specific spinal alignment adjustment. (A) Experimental skin marker locations attached over the respective spinous processes. (B) Approximation of intervertebral joint center locations (blue dots) by subtracting the marker-joint offsets from the external marker positions (red dots). Marker-joint offsets were obtained from virtual markers and joint centers in the generic model, after scaling the model to match the subject dimension. Underlying assumption was a vertebral orientation according to the normal vector of the external back profile (4th order polynomial in red). (C) Internal spine shape obtained from 4th order polynomial (in blue) by using predicted joint centers and a supporting posterior head marker center point. (D) Final predicted joint centers with predefined relative vertical spacing (according to the generic model) between intervertebral joints. (E) Final calculated joint orientation determined by the normal vector to the polynomial representing subject-specific spinal alignment. (For interpretation of the references to colour in this figure legend, the reader is referred to the web version of this article.)

Inverse kinematics calculations to obtain joint angles at each timepoint by solving a weighted least squares error problem. (2) Static optimization to estimate activity and force of the individual muscle fibers (using muscle force–length curve) by minimizing the sum of squared muscle activations (Herzog, 1987). (3) Compressive and AP shear joint reaction force estimations by solving the static equations for each timepoint and joint using the estimated muscle forces from the static optimization, experimental ground reaction forces and segmental masses.

To evaluate the differences between the generic and subject-specific model predictions as well as the OrthoLoad data, we performed pairwise comparisons of the continuous data using MATLAB and the package "spm1d" for one-dimensional Statistical Parametric Mapping (SPM; https://www.spm1d.org) (Pataky, 2012). Differences between the generic and subject-specific model predictions were thereby evaluated with two-tailed paired t-tests (SPM function: "spm1d.stats.ttest_paired"), whereas differences between model predictions and OrthoLoad data were evaluated with independent samples t-tests (SPM function: "spm1d.stats.ttest2"). The alpha level was set at 0.017 (Bonferroni-corrected).

3. Results

Mean L1/L2 compressive forces between the subject-specific and generic modeling approaches showed no differences for box lifting but slightly higher values for all other tasks during most of the movement cycles (Fig. 3). Mean L1/L2 AP shear forces resulting from the subject-specific scaling approach were higher for box lifting and chair rising but lower for stair climbing and walking (Fig. 4). Compared to the OrthoLoad data, the predicted compressive forces were considerably higher for both scaling approaches over all simulated activities (Fig. 3). AP shear forces during box lifting were considerably higher for the subject-specific but similar for the generic approach (Fig. 4). For chair rising, AP shear forces for both simulation approaches were similar during the first 40% and last 20% but considerably higher during 40–80% of the movement phase. For stair climbing and walking, both approaches resulted in increased posteriorly directed shear forces, with values resulting from the subject-specific approach being closer to the in vivo data as compared to the generic approach. Intersegmental kinematics for all spinal levels can be found in the electronic supplementary material.

4. Discussion

This study introduces a novel skin marker-based approach for modeling subject-specific spinal alignment, which enables subject-specific simulations of trunk muscle activity and spinal loading during various functional activities. Comparisons between predicted and in vivo measured L1/L2 intervertebral loading showed considerably higher compressive forces for both scaling approaches over all simulated activities, and AP shear forces that were closer or similar to the in vivo data for the generic approach during box lifting and chair rising and for the subject-specific approach during stair climbing and walking.

Even though the proposed approach aimed at the personalized prediction of internal spinal shape, it still heavily relies on the distances between markers and joint centers of the base models, which were simply set by drag and drop in the OpenSim graphical user interface and without considering the individualism among subjects with respect to these distances. In a next step, it might therefore be meaningful to implement linear regression models for a better approximation of the distances between markers and joint centers by variables such as gender, height, mass and age, and thus increase the subject-specificity of the model and potentially further improve skin marker-based IVJ center location and vertebral orientation predictions. A more sophisticated inclusion of marker-to-joint distance estimations already in the base

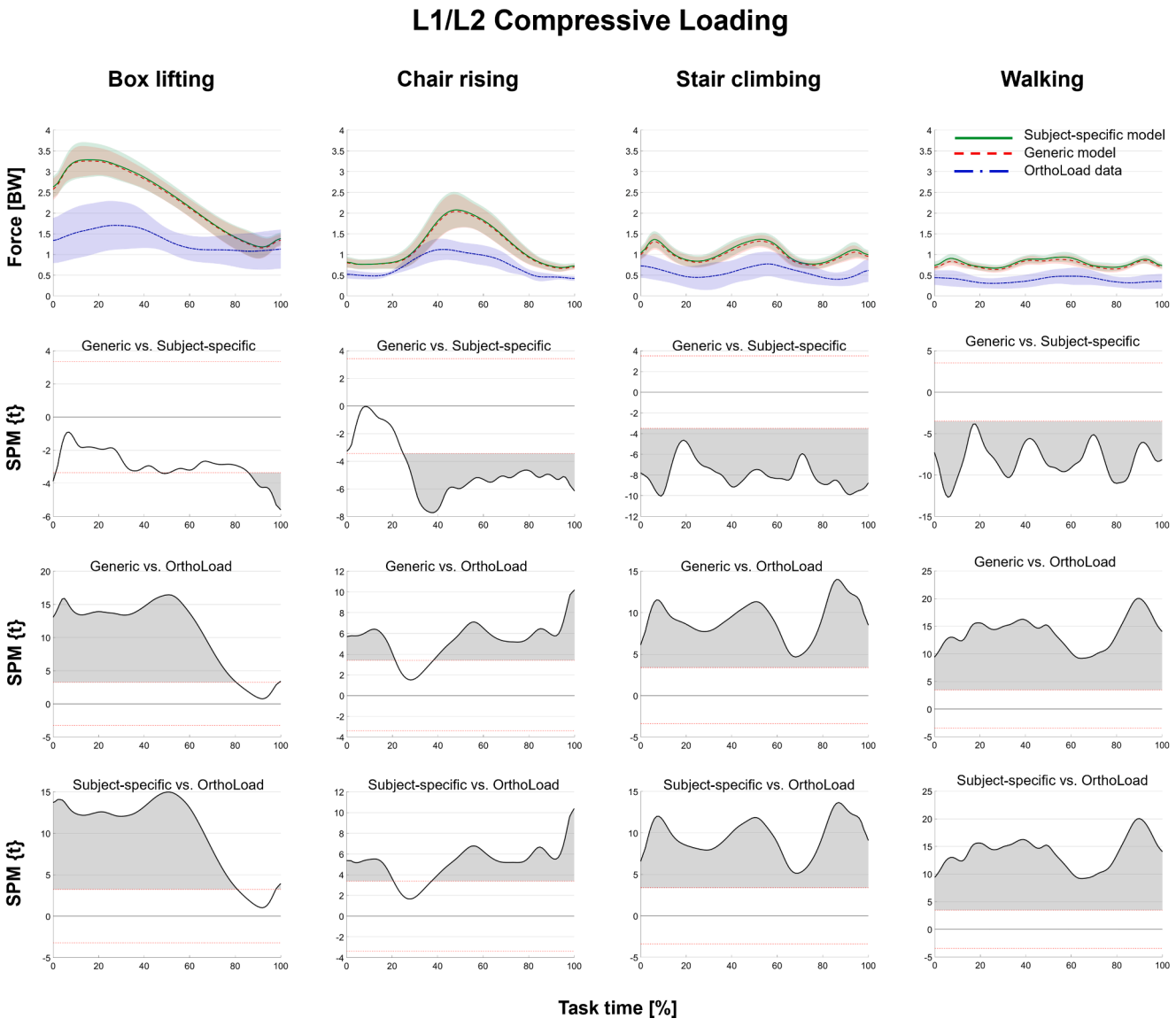

Fig. 3. First row: Mean compressive joint forces (±1 standard deviation) at the L1/L2 level during box lifting, chair rising, stair climbing and walking, derived from the OrthoLoad database (blue dash-dotted lines) as well as resulting from simulations with the generic (red dashed lines) and subject-specific models (green solid lines). Second to fourth rows: Results of the comparisons between the forces from the generic and subject-specific models as well as the OrthoLoad database using one-dimensional Statistical Parametric Mapping (SPM), with the red dotted lines indicating the critical thresholds for statistical significance at the $p = 0.017$ level and the gray shaded areas the supra-threshold clusters, where the t-value crosses the critical threshold indicating statistically significant differences. (For interpretation of the references to colour in this figure legend, the reader is referred to the web version of this article.)

model would hence be advised before generalizing the method. This particularly applies to modeled deformities or other conditions such as obesity.

Furthermore, despite the subject-specific spinal alignment adjustments, the models created with this method remain generic to some extent. To prevent large errors caused by inaccurate marker placements, the method does not adjust the vertical spacing of the vertebrae, which in turn might result in some non-negligible prediction errors. In addition, the use of only two markers (C7 and SACR) for scaling the whole torso including the length of the spine might lead to additional prediction errors. Due to different sacral orientations as well as the larger amount of soft tissue and less clearly identifiable bony landmarks in lower back / sacrum region, the placement of the SACR marker seems thereby to be particularly challenging. Using additional markers such as the ones placed on the posterior superior iliac spines ((R/L)PSI) to calculate the scaling factor might improve spinal height approximation, but the prediction of subject-specific vertebral morphometric features such as disc height, vertebral body height and transverse width will remain generic. Joint orientations are also generic by always being perpendicular to the spline at the corresponding joint location, as it is impossible to reliably derive orientations based on fewer skin markers than joints. From a computational point of view, such a simplification has advantages, as - similar to smoothening marker positions by the polynomial fitting - they ensure a certain amount of continuity in the arrangement of the spinal column, which increases the computational robustness of created models.

To confirm that the proposed subject-specific spinal alignment approach results in more accurate predictions of IVJ position and orientation as compared to using the alignment of the generic models, radiographic validation studies are needed. If possible, these studies should thereby always include simultaneous radiographic and motion capture measurements in order to minimize any errors emerging from different spinal postures between the measurements. In addition, the potential of the subject-specific approach might be best evaluated when

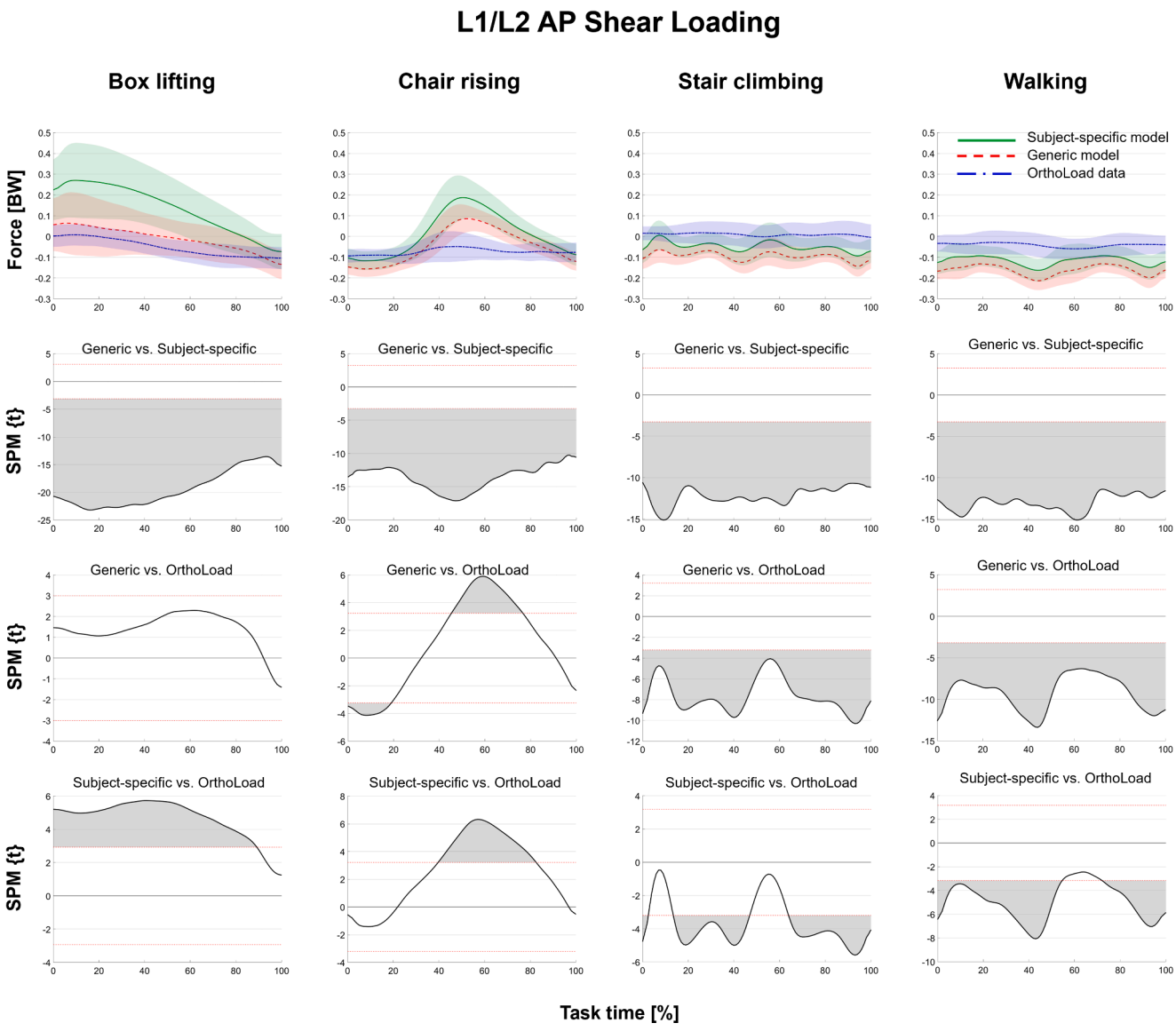

Fig. 4. First row: Mean AP shear joint forces (±1 standard deviation) at the L1/L2 level during box lifting, chair rising, stair climbing and walking, derived from the OrthoLoad database (blue dash-dotted lines) as well as resulting from simulations with the generic (red dashed lines) and subject-specific models (green solid lines). Second to fourth rows: Results of the comparisons between the forces from the generic and subject-specific models as well as the OrthoLoad database using one-dimensional Statistical Parametric Mapping (SPM), with the red dotted lines indicating the critical thresholds for statistical significance at the $p = 0.017$ level and the gray shaded areas the supra-threshold clusters, where the t-value crosses the critical threshold indicating statistically significant differences. (For interpretation of the references to colour in this figure legend, the reader is referred to the web version of this article.)

including a variety of sagittal plane spinal deformities as for example a thoracic hyperkyphosis, which can be observed in the context of physiologic age-related changes or as a result from pathologic conditions such as the Scheuermann disease.

The almost identical L1/L2 mean compressive forces resulting from the generically scaled models and the models with subject-specific spinal alignments gives the impression that the spinal alignment adjustments did not have any effect on intervertebral loading. However, when looking at the curves within the individual subjects, it becomes apparent that only a few subjects showed almost identical forces, while the others showed either slightly lower or higher forces (Fig. 5). However, as it can also be seen in Fig. 5, the spinal shapes of our measured healthy individuals were quite similar to the one of the generic model, which explains the only marginal differences between the loads predicted by the subject-specific and the generic approaches. It can be expected that these differences are larger in subjects with more pronounced spinal shape deviations.

Our models were able to estimate joint loading for the activities walking, running, chair rising, box lifting and stair climbing, without the need for task-specific tuning. However, the robustness of our models comes at the cost of adding numerous coordinate actuators (artificial torque generators) to the spinal joints, which provide support when the optimizer is unable to find a solution based on the modeled muscles. The torques generated by these actuators are not negligible, but in comparison with muscle-generated torques, their implementation seems adequate. During model development we ensured that the actuation limits were kept as low as possible, just high enough to ensure model convergence while avoiding excessive torques. Particularly with respect to missing an explicit soft-tissue representation in the model, the torque actuators can be considered a way to account for highly variable passive stiffness properties within the musculoskeletal system. Still, the lack of explicitly modeled soft tissue and negligence of other factors such as intra-abdominal pressure might partially explain the differences in joint loading observed between our model predictions and the in vivo

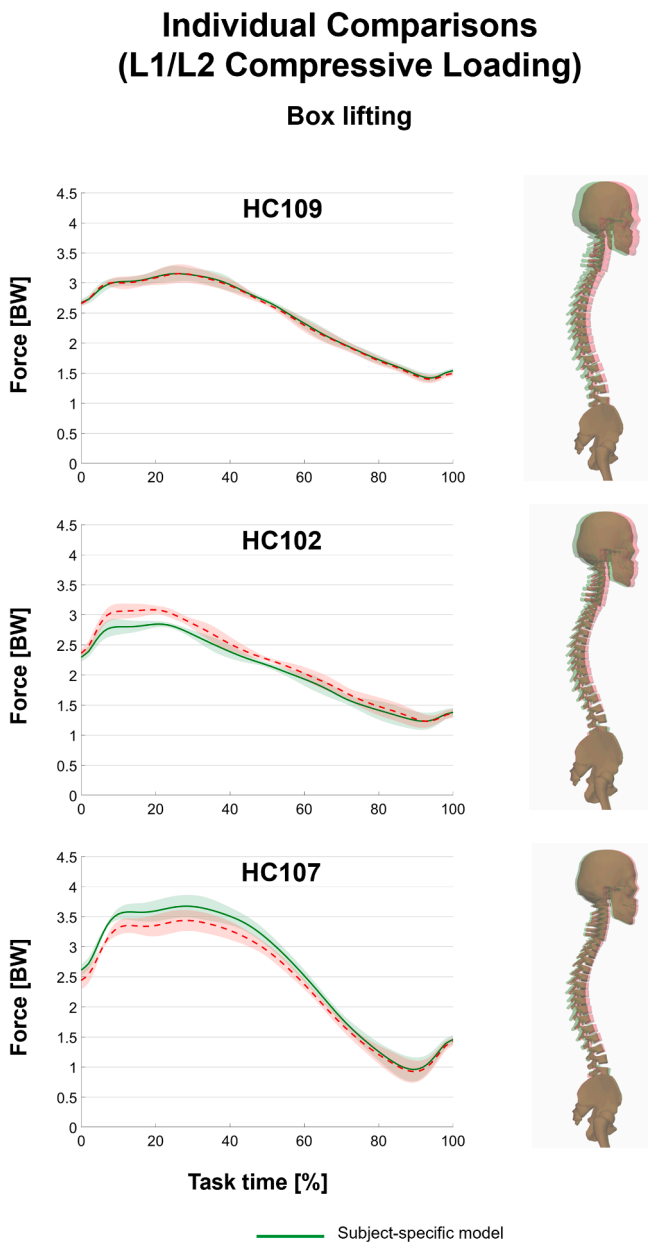

Fig. 5. Exemplary compressive joint forces at the L1/L2 level during box lifting for three selected subjects (mean ± 1 standard deviation of the five repetitions performed by each subject) resulting from simulations with the subject-specific (green solid lines) and generic models (red dashed lines). Forces were either almost identical (subject "HC109"), slightly lower (subject "HC102"), or higher (subject "HC107"). The overlapping skeletons next to the graphs illustrate the differences in spinal shapes between the subject-specific (green) and generic models (red). (For interpretation of the references to colour in this figure legend, the reader is referred to the web version of this article.)

measured data. Previous studies showed that incorporating these factors might lead to more accurate spinal loading estimations (Ghezelbash et al., 2018; Liu et al., 2019; Wang et al., 2019). Other possible explanations are the design of the instrumented implants and the fact that the in vivo measurements were based on spinal surgery patients, which most likely presented altered movement patterns as for example a reduced lumbar flexion during object lifting. In terms of implant design, the presence of the posterior external rods suggests that the sensors did not account for the entire load transferred through the vertebral body. On the other hand, our models did not include facet joints, which means that the entire load was transferred through the intervertebral disc. It can therefore be assumed that the "real" intersegmental loads probably lie somewhere in between the in vivo measurements and our model predictions.

In conclusion, we created OpenSim male and female musculoskeletal full-body models, which enable simulations of various functional activities. Moreover, we introduced a novel skin marker-based approach for subject-specific spinal alignment adjustments. Both models and code are freely available via the project-hosting platform SimTK. When implemented into standard model scaling workflows, it is expected to improve the accuracy of muscle activity and joint loading simulations, which is crucial for investigations of treatment effects or pathology-dependent deviations.

CRediT authorship contribution statement

Stefan Schmid: Writing – original draft, Methodology, Formal analysis, Data curation, Conceptualization. **Lukas Connolly:** Conceptualization, Data curation, Formal analysis, Methodology, Software, Writing – review & editing. **Greta Moschini:** Writing – review & editing, Software, Methodology. **Michael L. Meier:** Conceptualization, Funding acquisition, Supervision, Writing – review & editing. **Marco Senteler:** Writing – review & editing, Supervision, Methodology, Conceptualization.

Declaration of Competing Interest

The authors declare that they have no known competing financial interests or personal relationships that could have appeared to influence the work reported in this paper.

Acknowledgments

This research was supported by the Swiss National Science Foundation (SNSF, Bern, Switzerland; Grant-no.: 185123). Movement analysis was performed with support of the Swiss Center for Clinical Movement Analysis (SCMA). The authors thank Marina Hitz, Linard Filli, and Marc Bolliger from the SCMA for their support.

Appendix A. Supplementary data

Supplementary data to this article can be found online at https://doi.org/10.1016/j.jbiomech.2022.111102.

References

Anderson, F.C., Pandy, M.G., 1999. A Dynamic Optimization Solution for Vertical Jumping in Three Dimensions. Comput. Methods Biomech. Biomed. Eng. 2, 201–231.
Anderson, F.C., Pandy, M.G., 2001. Dynamic optimization of human walking. J. Biomech. Eng. 123, 381–390.
Bassani, T., Galbusera, F., 2018. Musculoskeletal Modeling. In: Galbusera, F., Hans-Joachim, W. (Eds.), Biomechanics of the Spine. Basic Concepts, Spinal Disorders and Treatments. Academic Press, Cambridge, MA, USA.
Bassani, T., Stucovitz, E., Qian, Z., Briguglio, M., Galbusera, F., 2017. Validation of the AnyBody full body musculoskeletal model in computing lumbar spine loads at L4L5 level. J. Biomech. 58, 89–96.
Beaucage-Gauvreau, E., Robertson, W.S.P., Brandon, S.C.E., Fraser, R., Freeman, B.J.C., Graham, R.B., Thewlis, D., Jones, C.F., 2019. Validation of an OpenSim full-body model with detailed lumbar spine for estimating lower lumbar spine loads during symmetric and asymmetric lifting tasks. Comput. Methods Biomech. Biomed. Eng. 22, 451–464.
Bruno, A.G., Bouxsein, M.L., Anderson, D.E., 2015. Development and Validation of a Musculoskeletal Model of the Fully Articulated Thoracolumbar Spine and Rib Cage. J. Biomech. Eng. 137, 81003.
Bruno, A.G., Burkhart, K., Allaire, B., Anderson, D.E., Bouxsein, M.L., 2017. Spinal Loading Patterns From Biomechanical Modeling Explain the High Incidence of Vertebral Fractures in the Thoracolumbar Region. J. Bone Mineral Res.: Official J. Am. Soc. Bone Mineral Res. 32, 1282–1290.
Burkhart, K., Grindle, D., Bouxsein, M.L., Anderson, D.E., 2020. Between-session reliability of subject-specific musculoskeletal models of the spine derived from optoelectronic motion capture data. J. Biomech. 112, 110044.

Christophy, M., Faruk Senan, N.A., Lotz, J.C., O'Reilly, O.M., 2012. A musculoskeletal model for the lumbar spine. Biomech. Model. Mechanobiol. 11, 19–34.
de Zee, M., Hansen, L., Wong, C., Rasmussen, J., Simonsen, E.B., 2007. A generic detailed rigid-body lumbar spine model. J. Biomech. 40, 1219–1227.
Delp, S.L., Anderson, F.C., Arnold, A.S., Loan, P., Habib, A., John, C.T., Guendelman, E., Thelen, D.G., 2007. OpenSim: open-source software to create and analyze dynamic simulations of movement. IEEE Trans. Bio-med. Eng. 54, 1940–1950.
Delp, S.L., Loan, J.P., Hoy, M.G., Zajac, F.E., Topp, E.L., Rosen, J.M., 1990. An interactive graphics-based model of the lower extremity to study orthopaedic surgical procedures. IEEE Trans. Bio-med. Eng. 37, 757–767.
Ghezelbash, F., Eskandari, A.H., Shirazi-Adl, A., Arjmand, N., El-Ouaaid, Z., Plamondon, A., 2018. Effects of motion segment simulation and joint positioning on spinal loads in trunk musculoskeletal models. J. Biomech. 70, 149–156.
Glover, N.A., Kakar, R.S., Chaudhari, A.M.W., 2021. Effects of spinal coupling and marker set on tracking of spine models during running. J. Biomech. 116, 110217.
Herzog, W., 1987. Individual muscle force estimations using a non-linear optimal design. J. Neurosci. Methods 21, 167–179.
Ignasiak, D., Dendorfer, S., Ferguson, S.J., 2016. Thoracolumbar spine model with articulated ribcage for the prediction of dynamic spinal loading. J. Biomech. 49, 959–966.
Ignasiak, D., Rüeger, A., Sperr, R., Ferguson, S.J., 2018. Thoracolumbar spine loading associated with kinematics of the young and the elderly during activities of daily living. J. Biomech. 70, 175–184.
Liu, T., Khalaf, K., Adeeb, S., El-Rich, M., 2019. Numerical Investigation of Intra-abdominal Pressure Effects on Spinal Loads and Load-Sharing in Forward Flexion. Front. Bioeng. Biotechnol. 7.
Niggli, L.A., Eichelberger, P., Bangerter, C., Baur, H., Schmid, S., 2021. Between-session reliability of skin marker-derived spinal kinematics during functional activities. Gait Posture 85, 280–284.
Pataky, T.C., 2012. One-dimensional statistical parametric mapping in Python. Comput. Methods Biomech. Biomed. Eng. 15, 295–301.
Raabe, M.E., Chaudhari, A.M.W., 2018. Biomechanical consequences of running with deep core muscle weakness. J. Biomech. 67, 98–105.
Schmid, S., Bruhin, B., Ignasiak, D., Romkes, J., Taylor, W.R., Ferguson, S.J., Brunner, R., Lorenzetti, S., 2017. Spinal kinematics during gait in healthy individuals across different age groups. Hum. Mov. Sci. 54, 73–81.
Schmid, S., Burkhart, K.A., Allaire, B.T., Grindle, D., Anderson, D.E., 2020. Musculoskeletal full-body models including a detailed thoracolumbar spine for children and adolescents aged 6–18 years. J. Biomech. 102, 109305.
Seth, A., Sherman, M., Reinbolt, J.A., Delp, S.L., 2011. OpenSim: a musculoskeletal modeling and simulation framework for in silico investigations and exchange. Proc. IUTAM 2, 212–232.
Suter, M., Eichelberger, P., Frangi, J., Simonet, E., Baur, H., Schmid, S., 2020. Measuring lumbar back motion during functional activities using a portable strain gauge sensor-based system: A comparative evaluation and reliability study. J. Biomech. 100, 109593.
Wang, K., Wang, L., Deng, Z., Jiang, C., Niu, W., Zhang, M., 2019. Influence of passive elements on prediction of intradiscal pressure and muscle activation in lumbar musculoskeletal models. Comput. Methods Programs Biomed. 177, 39–46.
Yamaguchi, G.T., Zajac, F.E., 1989. A planar model of the knee joint to characterize the knee extensor mechanism. J. Biomech. 22, 1–10.